Developing the Powder Metallurgy

Mechanism analysis of liquid - liquid doping and fabrication of high properties of W - Zr(Y)O_2 alloys

Fangnao Xiao [a, b, c], Thierry Barriere [a], Gang Cheng [b], Qiang Miao [c]

a. FEMTO-ST Institute, CNRS/UFC/ENSMM/UTBM, Department of Applied Mechanics, Besançon, France

b. INSA CVL, Univ. Tours, Univ. Orléans, LaMé, 3 rue de la Chocolaterie, Blois Cedex, France

c. College of Material Science and Technology, Nanjing University of Aeronautics and Astronautics, Nanjing, China

Developing the Powder Metallurgy

Outline

EURO PM2020 VIRTU@L CONGRESS

- Introduction
- Mechanism of liquid-liquid doping
- Microstructure and properties of alloys
- Conclusions and perspectives

UNIVERSITé DE FRANCHE-COMTé · CNRS · ensmm · utbm · UBFC UNIVERSITE BOURGOGNE FRANCHE-COMTE · INSA INSTITUT NATIONAL DES SCIENCES APPLIQUÉES CENTRE VAL DE LOIRE · LaMé Laboratoire de Mécanique Gabriel Lamé · NUAA

1. Introduction

Innovative oxide particles strengthened W alloys

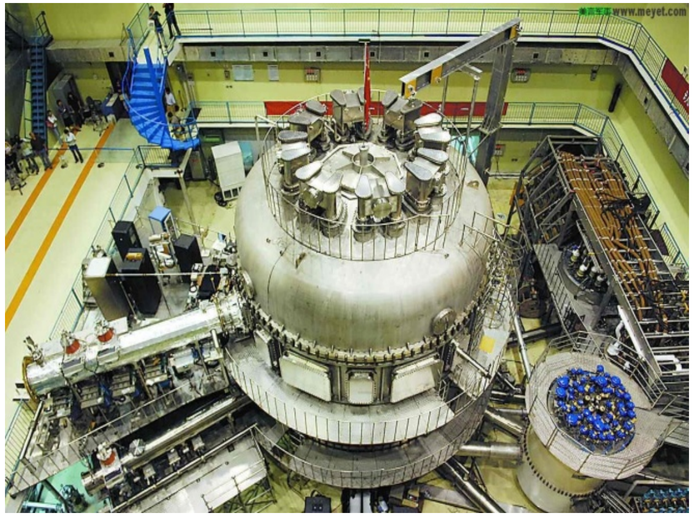

Traditional solid-solid / liquid doping processes

1. Uneven particle distribution, larger oxide particles;
2. Low-temperature and recrystallization embrittlement.

Research objectives

1. Nanosized oxide particles (< 500 nm) uniformly distributed within W grains;
2. Low ductile-brittle transition temperature (< 150 ℃) and high recrystallization temperature (> 1400 ℃).

2. Mechanism of liquid-liquid doping processes

Existence forms and reaction mechanisms of polytungstate ions

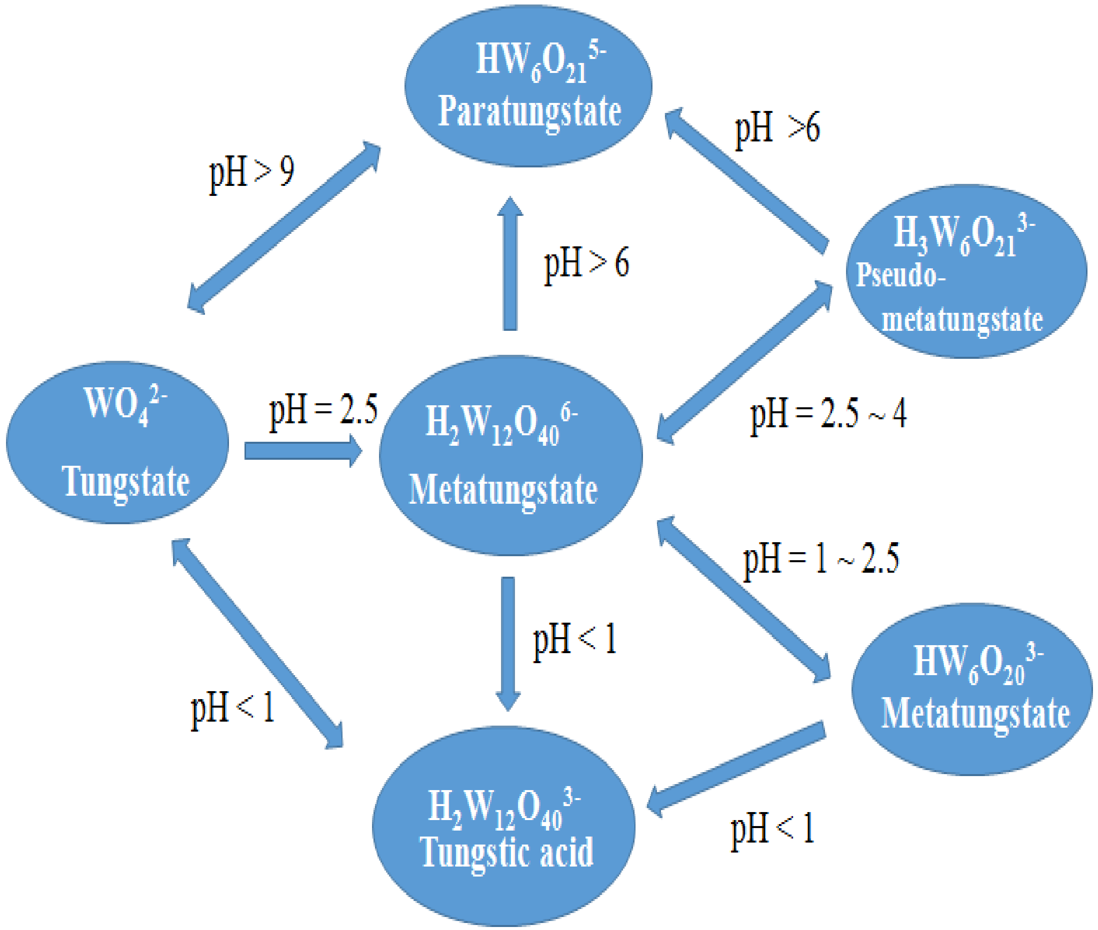

Reversible reaction equations	Reaction products	Common names
$(H_2W_{12}O_{40})^{6-}+6H^{+}+32H_2O=12(H_2WO_4\cdot 2H_2O)$	$H_2WO_4\cdot 2H_2O$	Tungstic acid
$H_2W_{12}O_{40}^{6-}+H^{+}=HW_{12}O_{39}^{5-}+H_2O$	$H_2W_{12}O_{40}^{6-}$ /$HW_{12}O_{39}^{5-}$	Metatungstate
$HW_{12}O_{39}^{5-}+2H_2O+OH^{-}=2(H_3W_6O_{21})^{3-}$	$(H_3W_6O_{21})^{3-}$	Pseudo-AMT
$(H_3W_6O_{21})^{3-}+2OH^{-}=(HW_6O_{21})^{5-}+2H_2O$	$(HW_6O_{21})^{5-}$	Paratungstate
$(HW_6O_{21})^{5-}+3H_2O+7OH^{-}=6(HWO_4)^{-}+H^{+}+7OH^{-}=6WO_4^{2-}+7H^{+}+7OH^{-}$	WO_4^{2-}	Tungstate ion

Liquid-liquid doping techniques for preparing $Zr(Y)O_2$ doped W powders

EURO PM2020 VIRTU@L CONGRESS

Hydrothermal method

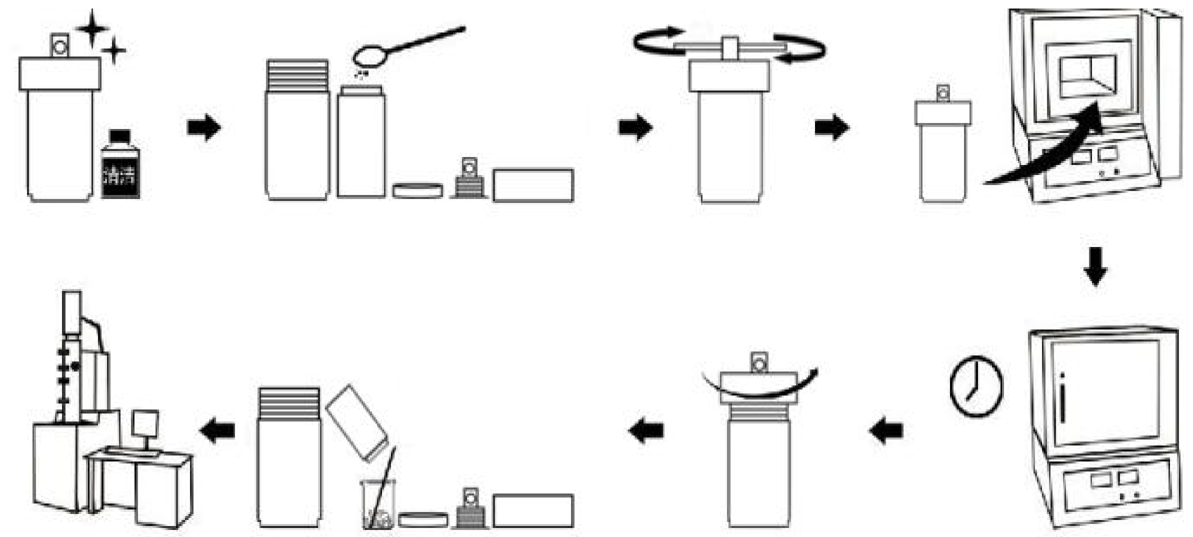

Hydrothermal reaction: 170 ℃

Duration: 12 hours

Azeotropic distillation method

Bath Temp.: 100 ℃

Dispersant: Alcohol + n-butyl alcohol

Sol-gel method

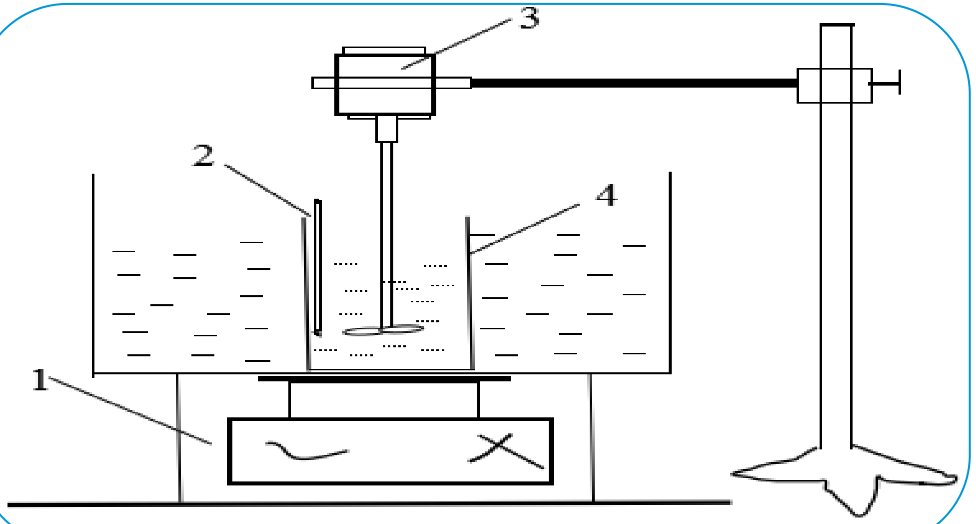

1 - Water bath
2 - Thermometer
3 - Digital stirring
4 - Beaker

Morphologies of precursors synthesized by three different doping processes

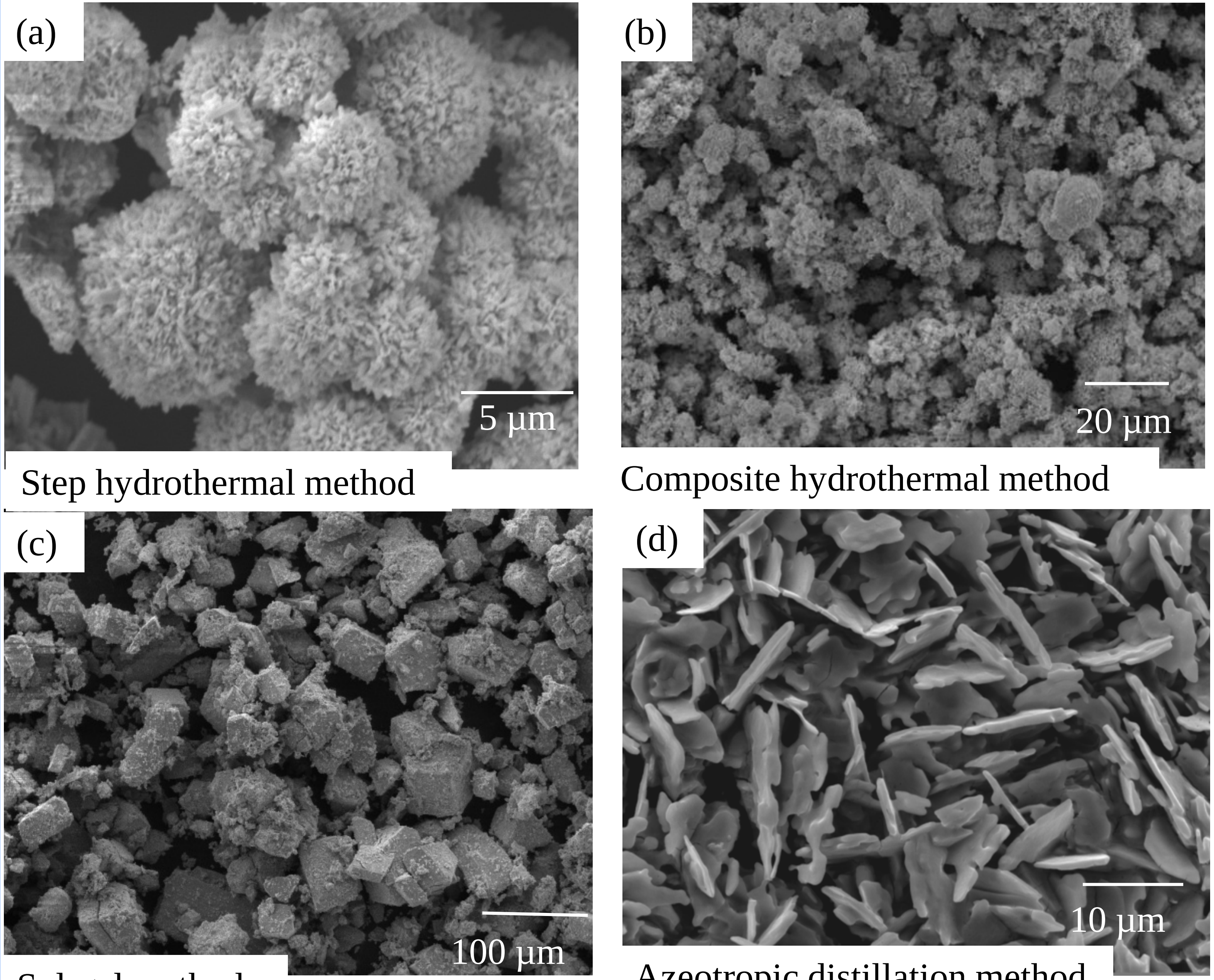

(a) Step hydrothermal method
(b) Composite hydrothermal method
(c) Sol-gel method
(d) Azeotropic distillation method

Precursors' morphologies:
(a) Microsphere;
(b) Loose;
(c) Angularity;
(d) Sheet.

Formation mechanism of doped precursor powders

1. Synthetization analysis of h-HATB powder by hydrothermal method

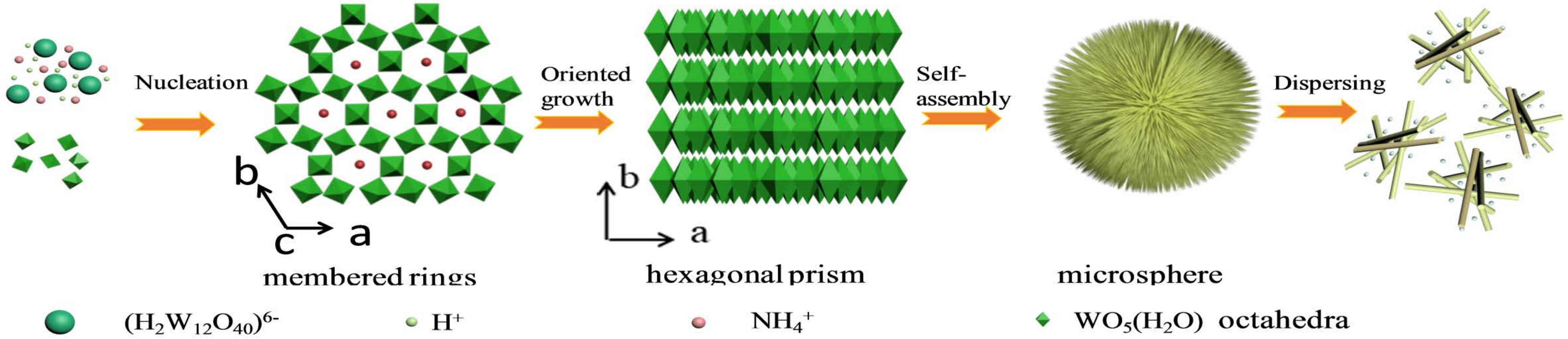

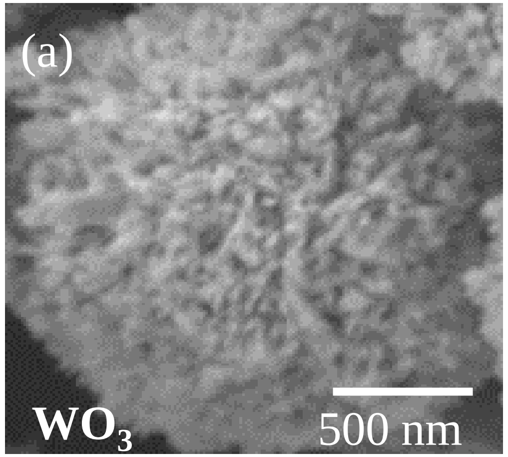

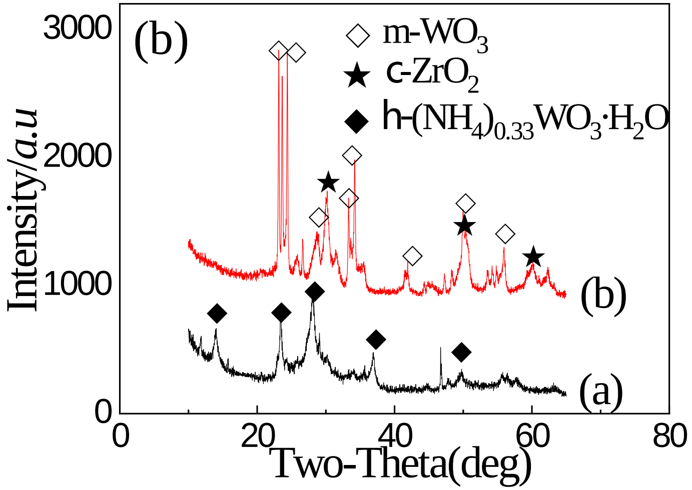

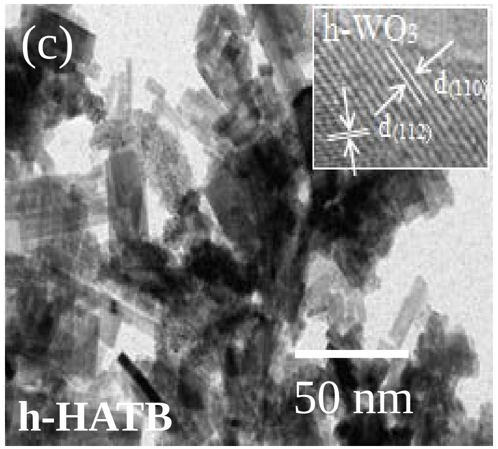

F. N. Xiao et al., J Alloy Compd. 843 (2020) 156059

Experimental observation of the synthetization of h-HATB

Formation mechanism of doped precursor powders

EURO PM2020 VIRTU@L CONGRESS

2. Synthetization analysis of precursor powder by azeotropic method

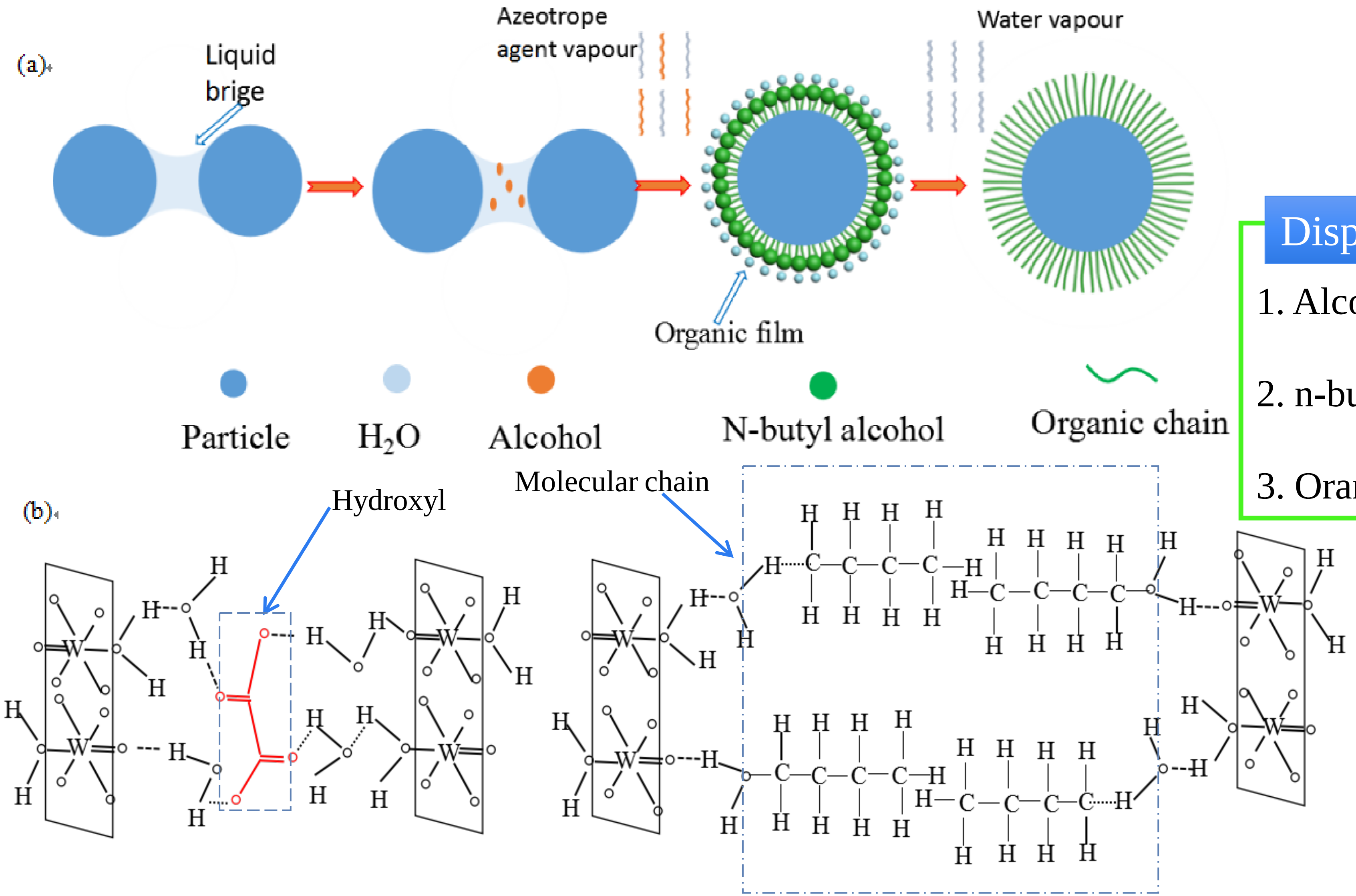

Dispersing process

1. Alcohol removing water;
2. n-bulty covering particles;
3. Oranic chain replacing hydroxly.

F. N. Xiao et al., J Alloy Compd. 708 (2017) 202-212

Morphologies of W- $Zr(Y)O_2$ powders reduced after 900 ℃ for 2 h

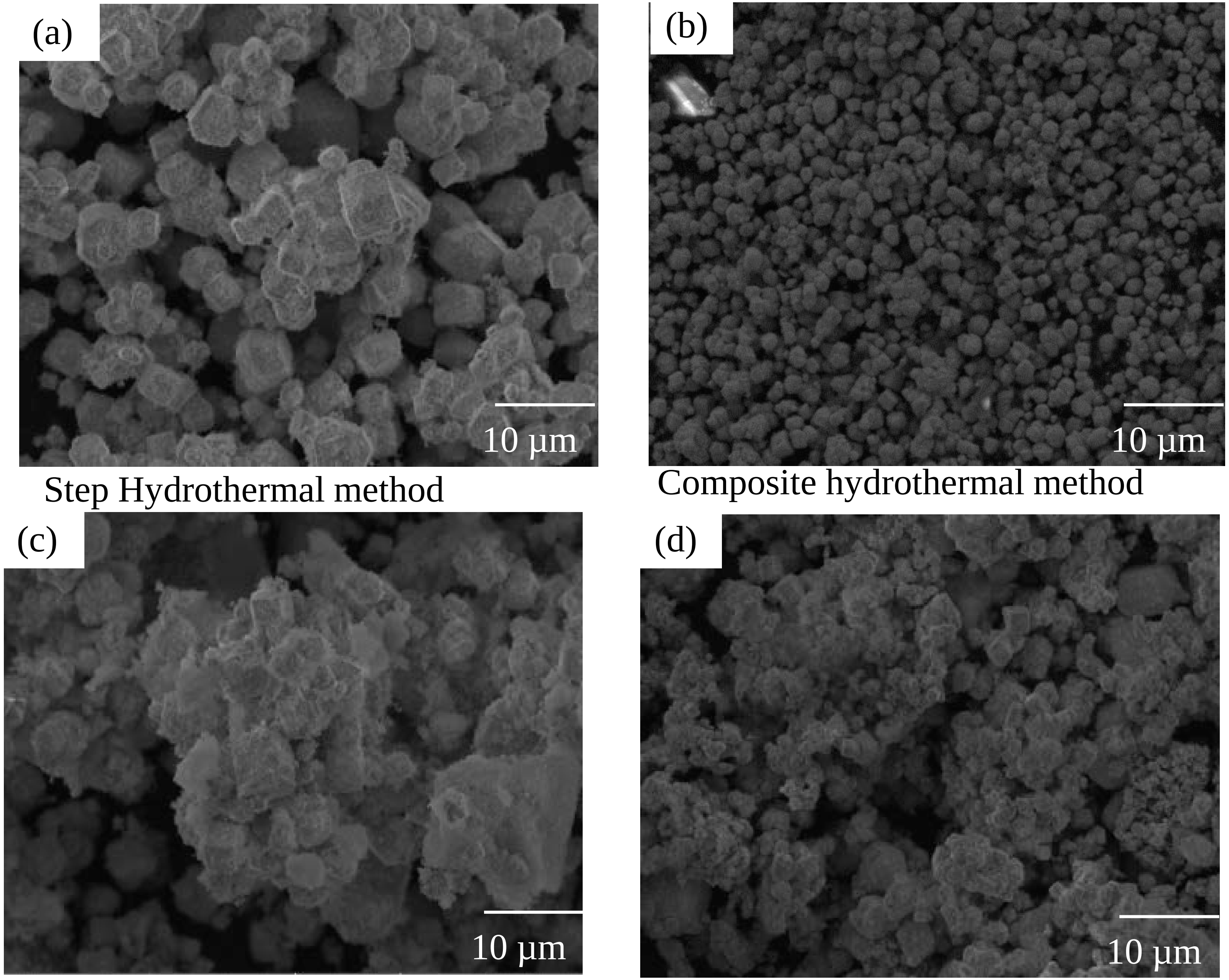

Step Hydrothermal method

Composite hydrothermal method

Sol-gel method

Azeotropic distillation method

1. Preserving the precursor' morphologies;

2. More uniformed – size and highly dispersed powders in Fig. b

F. N. Xiao et al., J Alloy Compd. 843 (2020) 156059

3. Microstructure and properties of Z(Y)O_2 strengthened W alloy

Description of innovative liquid – liquid doping process with optimal parameters

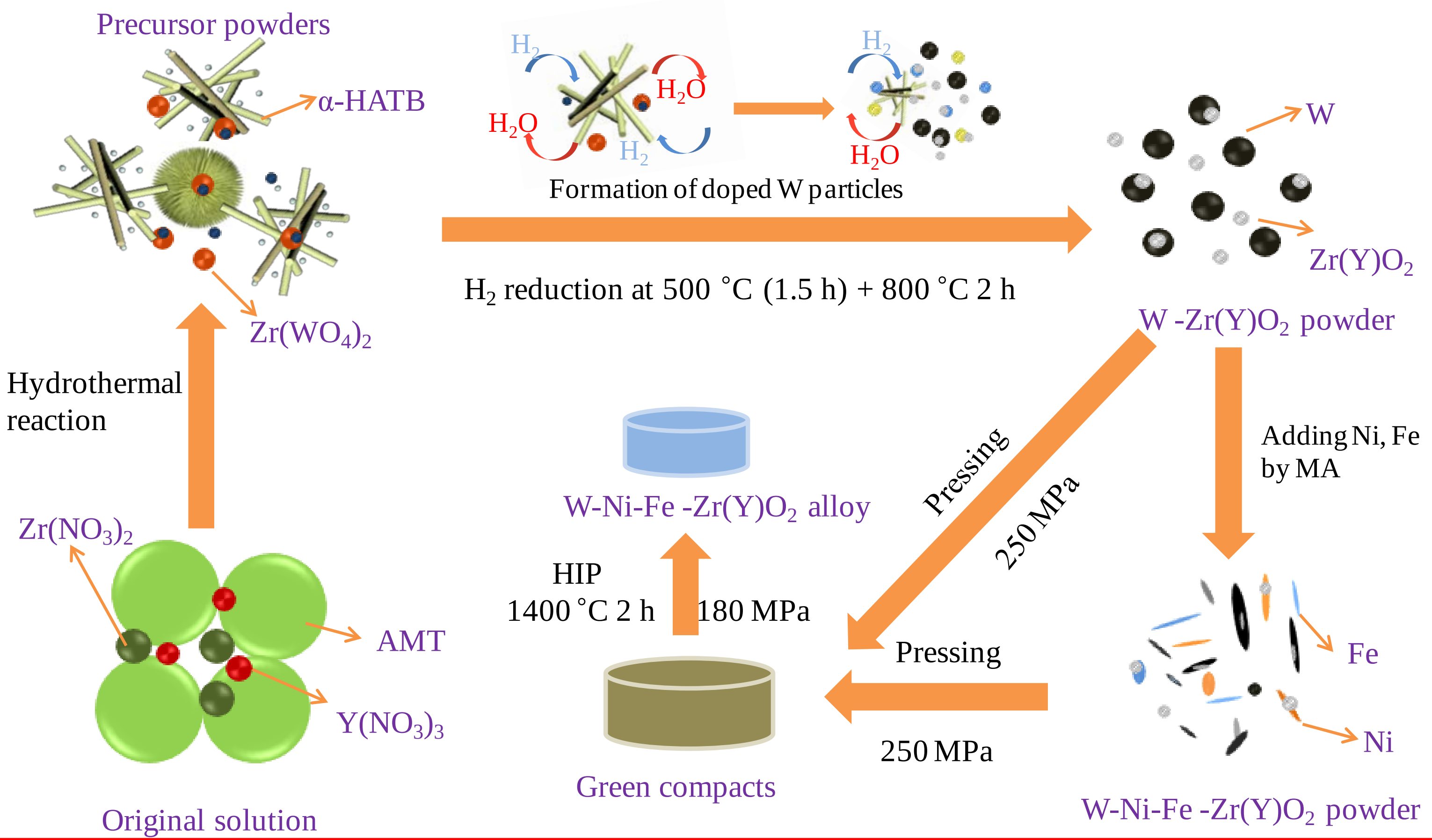

Ionic reaction mechanisms:

1. $2Zr^{4+} + W_{12}O_{40}^{8-} = 8WO_3\downarrow + 2Zr(WO_4)_2\downarrow$

2. $(H_2W_{12}O_{40})^{6-} + 6H^+ + 32H_2O = 12(H_2WO_4 \cdot 2H_2O)$

UNIVERSITé DE FRANCHE-COMTé cnrs ensmm utbm UBFC INSA INSTITUT NATIONAL DES SCIENCES APPLIQUÉES CENTRE VAL DE LOIRE LaMé Laboratoire de Mécanique Gabriel Lamé

Microstructure of the advanced material

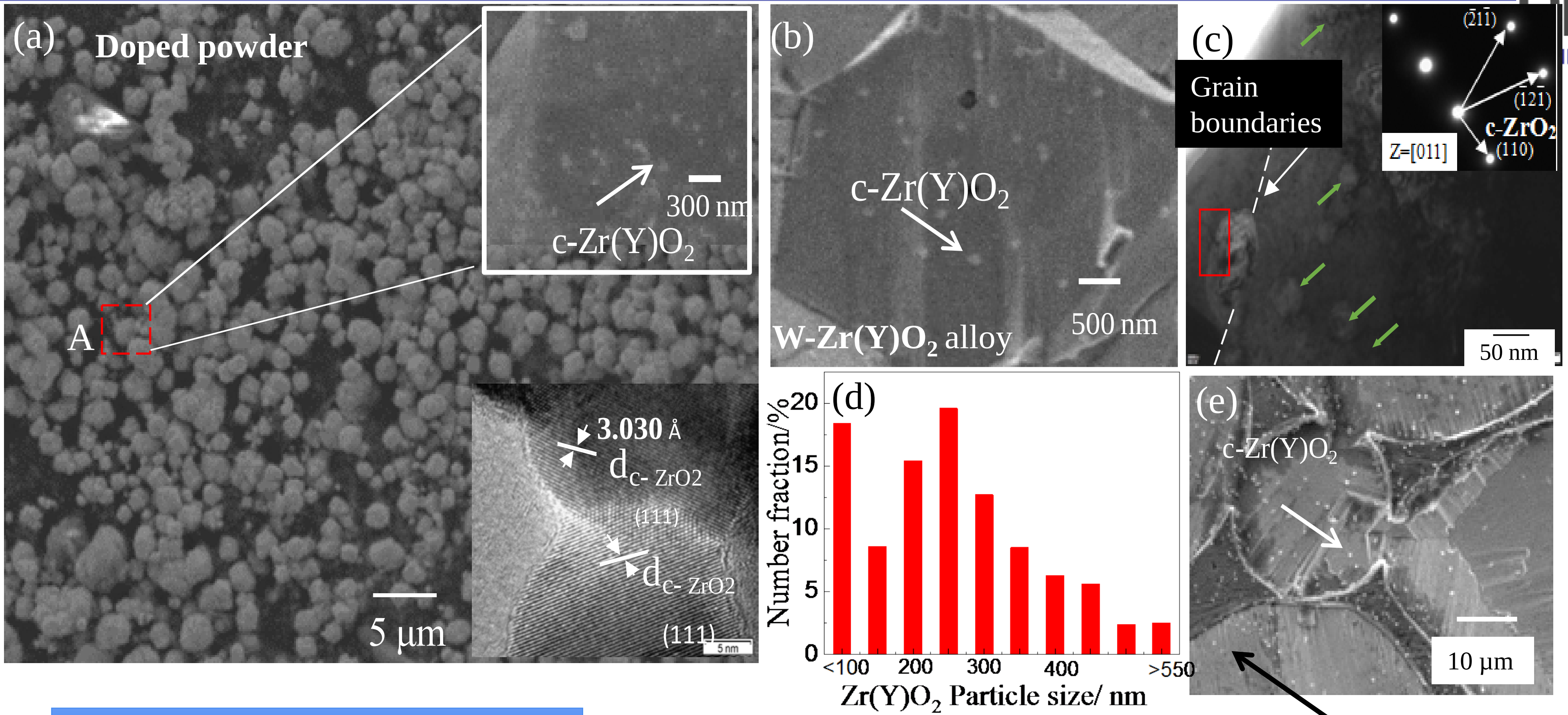

W-Ni-Fe-Zr(Y)O_2 alloy

Microstructure characterization

1. Highly dispersed doped powders, shown in Fig. (a);
2. 90% of particles distributed within W grains, shown in Fig. (b) and (e);
3. 85% of Zr(Y)O_2 particles are less than 300 nm in size, shown in Fig. (d).

F. N. Xiao et al., J. Alloy Compd. 774 (2019) 210–221

Comparison with state-of-the-art review

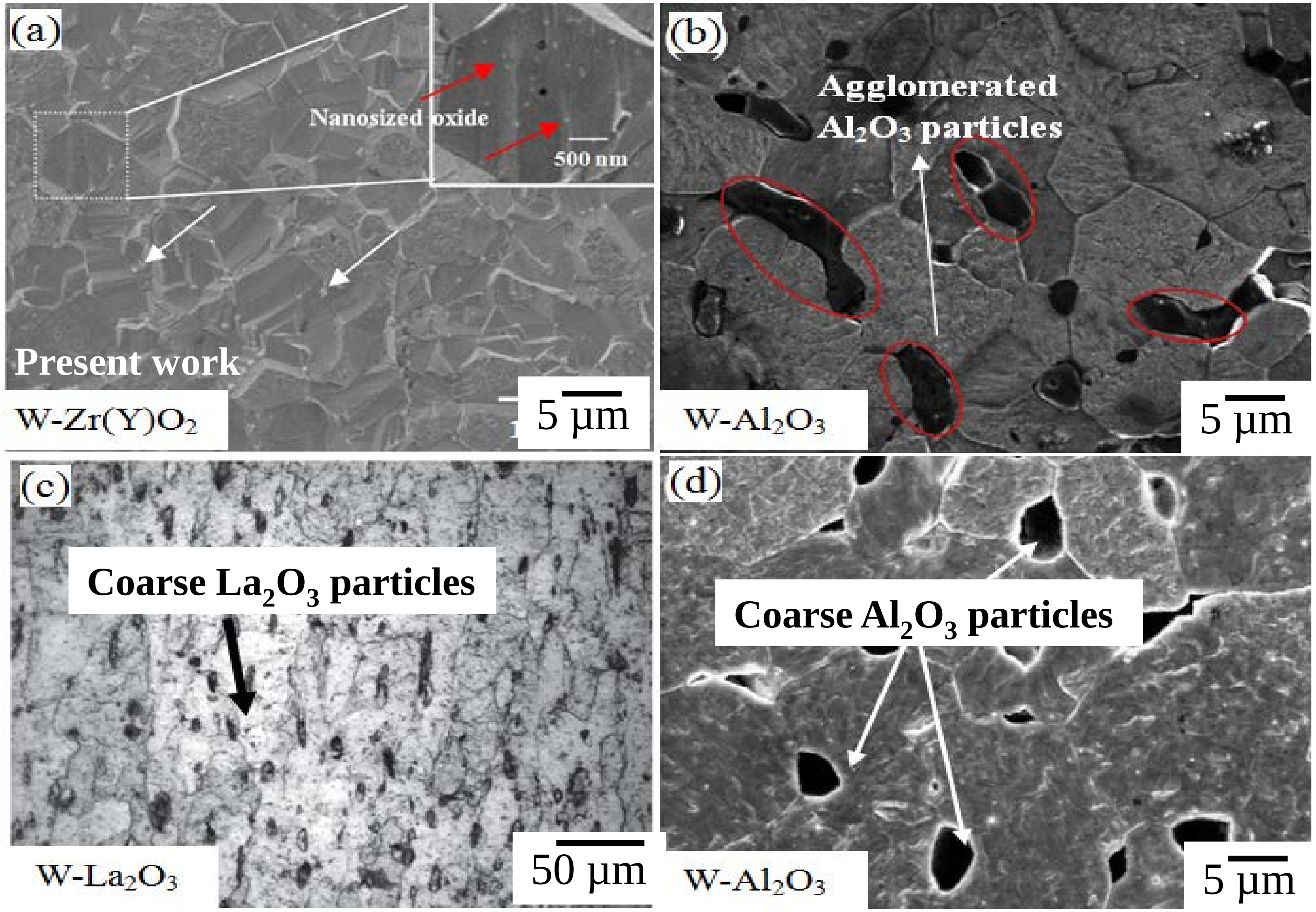

Main characteristic of the advanced W alloys

1. The oxide particle are smallest;
2. More oxide particles distributed within W grains;
3. The distribution of oxide particles are more uniform.

References

(a) Present work;
(b) C. J. Wang, J. Refract. Met. Hard Mater. 84 (2020) 105082;
(c) Y. Shen, J. Nucl. Mater. 455 (2014) 234-241;
(d) M. A. Yar, J. Nucl. Mater. 412 (2011) 227-232.

Comparison of microstructure and properties of ODS-W alloys

Doping process	Sintering Process	Alloy	W grain size (μm)	Oxide size (μm)	Relative density (%)	Microhardness /HV	Refs.
L - L	SPS	W-6vol% Al_2O_3	3.64	>1.0	94.96	347.39	[35]
	SPS	W-2.5%ZrO_2	4.65	2.5	99.6	480	[36]
	VD	W-2.5%ZrO_2	40-80	1.5	98.7	-	[37]
	VD	W-La_2O_3	50	3	-	-	[38]
L - S[a*]	SPS	W-0.9wt%La_2O_3	-	2	94	406	[39]
	SPS	W-1.0%Y_2O_3	2.3	Nanosize (Uneven)	92	423	[40]
	HIP	W-1%La_2O_3	-	>5	90.6	-	[41]
S - S	HIP	W-Ti-0.5%Y_2O_3	2-5	>1.5	-	-	[42]
	SPS	W-5%HfO_2	11.6	>5	94.5	440	[43]
Novel process	**HIP**	**W-0.5%Zr(Y)O_2**	**4.67± 0.5**	**0.25 ± 0.05**	**96.7 ± 0.2**	**472 ± 10**	**Present**

Conclusion

1. Smallest particles size;
2. Medium properties.

F. N. Xiao et al., J Alloy Compd. 843 (2020) 156059

Comparison with state-of-the-art review

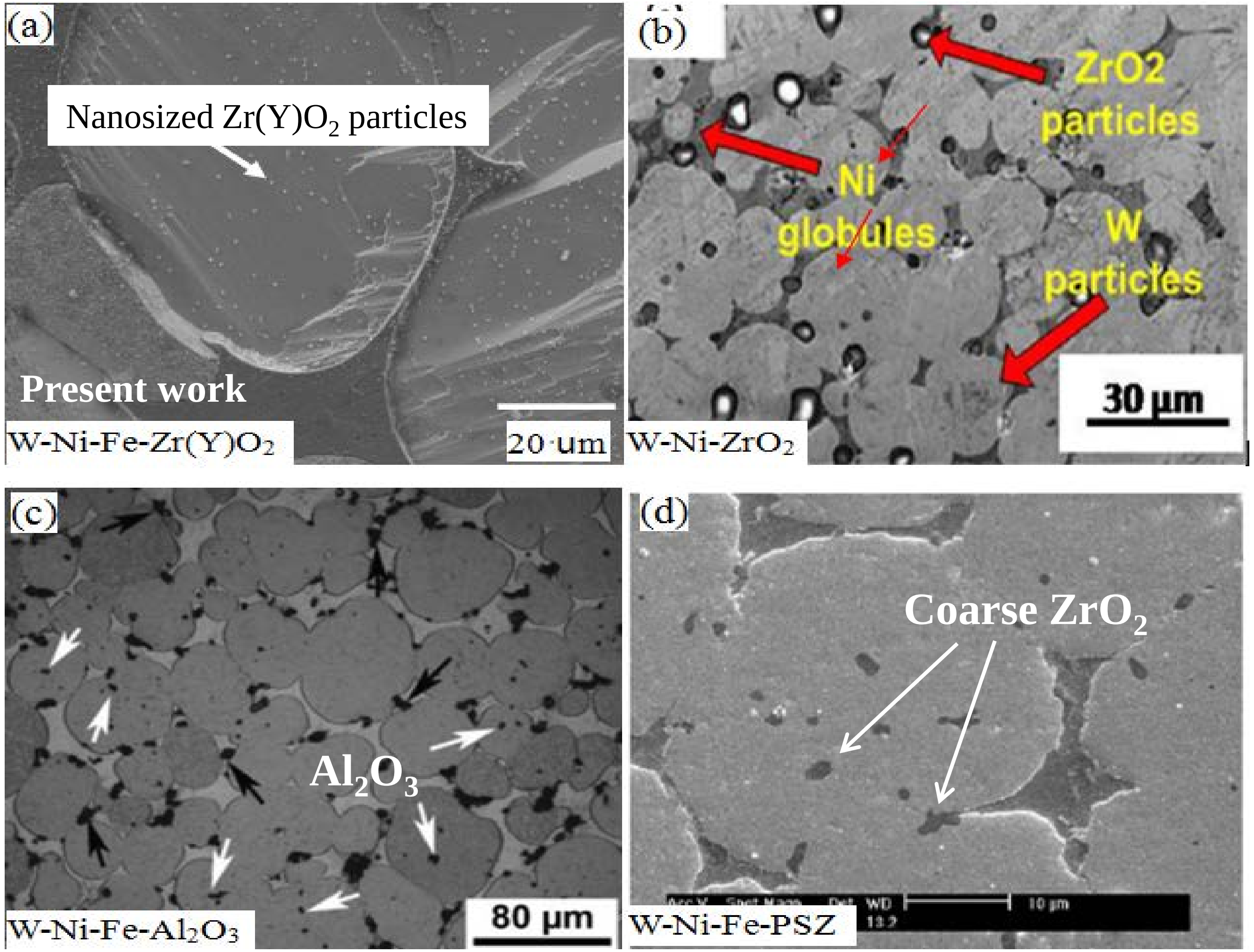

Main characteristic of my prepared heavy W alloy

1. The oxide particle are smaller;
2. Most $Zr(Y)O_2$ distributed within W grains;
3. The distribution of oxide particles are more uniform.

References

(a) Present work;
(b) W. M.R. Daoush Mater. Sci. Eng. A. 2016, 47(5): 2387-2395;
(c) K. H. Lee, J. Alloy. Compd. 2007, 434: 433-436;
(d) K. Hu, Mater. Sci. Eng. A. 2015, 636: 452-458.

Comparison of microstructure and properties of ODS-heavy W alloys

Heavy W alloy	Sintering process	RD/%	Grain size/μm	Particle size/μm	Hardness/ HV	Refs.
W–Ni-Fe–0.3PSZ	1480 ° C (1h)	-	18	0.8	-	[49]
W–Ni-Fe-1Al_2O_3		98.3	36.8	7	-	[52]
W–Ni-Fe–xY_2O_3	1485° C (1h)	99.1	19.5	0.6 - 1.3	-	[10]
W-Ni-ZrO_2	1500° C (1h)	93.5	~25	3 - 5	333	[50]
W-Ni-Fe-Co-Y_2O_3	1450° C (1h)	94.1	12	>0.6	425	[44]
94W-4.56Ni-1.14Fe-Y_2O_3	1485° C (1h)	99.0	15	0.65	-	[53]
Previous W-ODS	SPS/HIP	<99.9	<10	1 - 5	406 - 480	[27]
93W-4.9Ni-2.1Fe-Zr(Y)O_2	1520° C (2.5h)	99.2	26	0.2 - 1	402	[47]
$WHA_{0.75}$	**1400° C (2.5h)**	**99.2 ± 0.1**	**25 ± 2**	**0.2 - 1**	**402 ± 10**	**Present**

Conclusion

1. Finer particles;
2. Larger grain size;
3. Limited grain refinement.

F. N. Xiao et al., J Alloy Compd. 2020, 843: 156059

TEM analysis of HIP sintered W-Ni-Fe-ZrO_2 alloys

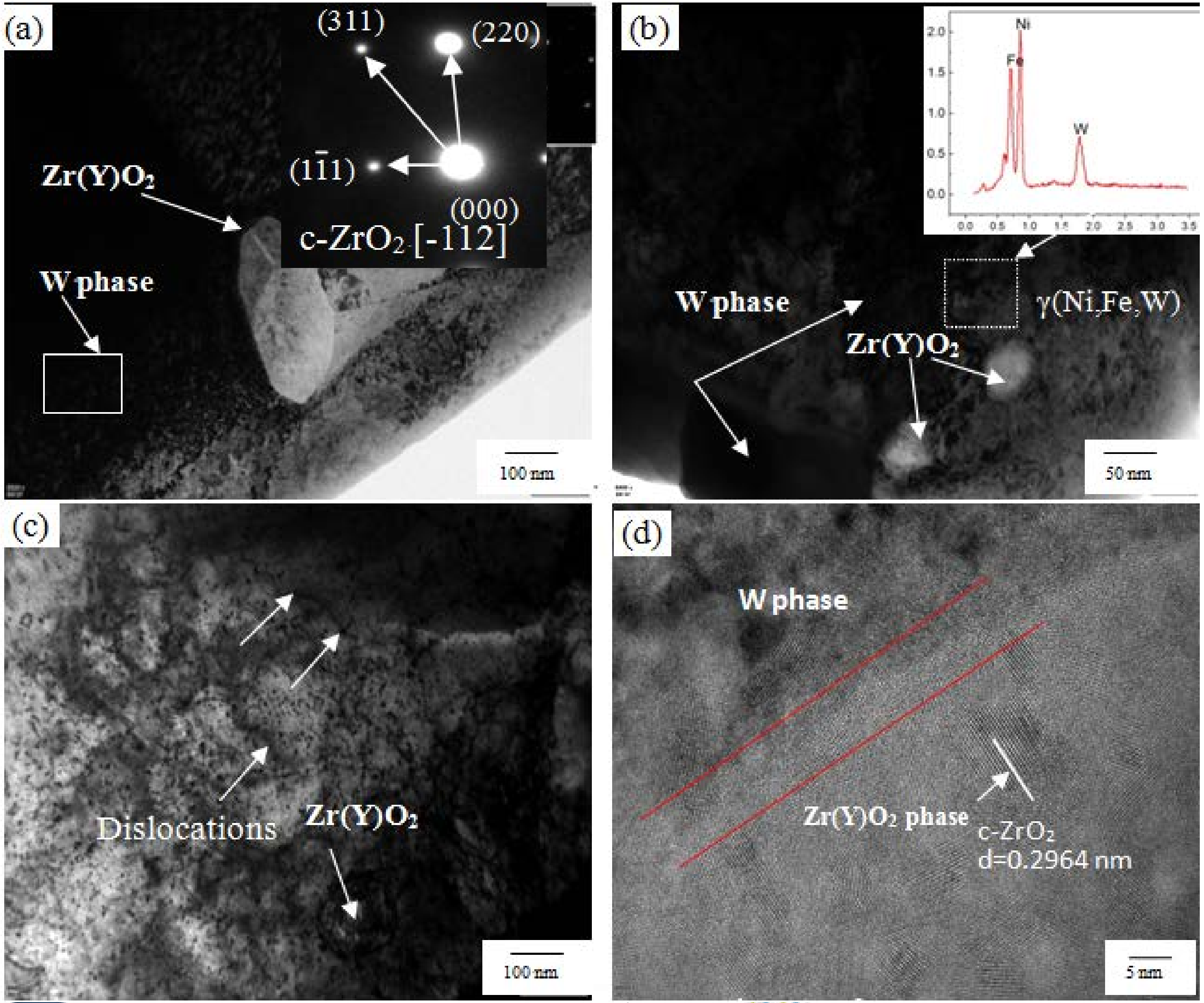

Conclusion

1. Cubic structure of $Zr(Y)O_2$;
2. Well - bonded interface.

Developing the Powder Metallurgy

Comparison of properties with state-of-the-art review

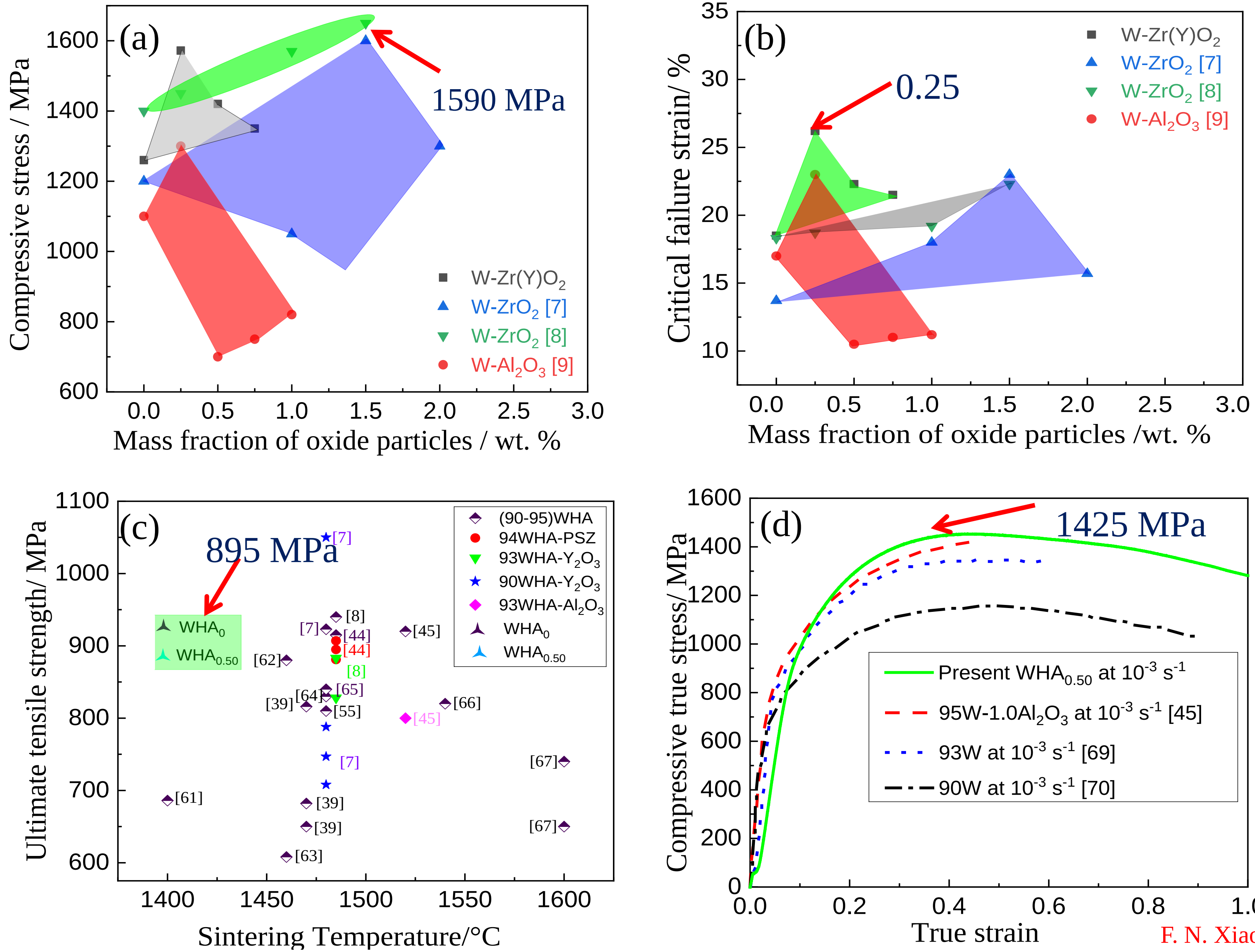

W-Zr(Y)O_2 alloy in fig (a, b)

1. High compressive strength;
2. High critical failure strain;
3. Higher than published alloys.

93W-Zr(Y)O_2 alloy in fig (c, d)

1. Higher tensile strength;
2. Compressive strength.

F. N. Xiao et al., J Alloy Compd. 2020, 824:153894

Mechanical properties of W-Zr(Y)O_2 alloy at high temperatures

Objective: **Arrhenius model was used to identify the compressive behaviours of the W-Zr(Y)O_2 alloy.**

$$Z = A\,[\sinh(\alpha\sigma)]^n$$

$$\downarrow$$

$$\ln Z = \ln A + n \ln[\sinh(\alpha\sigma)]$$

$$\downarrow$$

$$\ln \dot{\varepsilon} = \ln A + n \ln[\sinh(\alpha\sigma)]$$

$$\mathrm{AARE} = \frac{1}{N}\sum_i^N \left|\frac{(\sigma_e{}^i - \sigma_p{}^i)}{\sigma_e{}^i}\right| \times 100\%$$

$$\alpha = A_0 + A_1\varepsilon + A_2\varepsilon^2 + A_3\varepsilon^3 + A_4\varepsilon^4 + A_5\varepsilon^5 + A_6\varepsilon^6$$

$$n = B_0 + B_1\varepsilon + B_2\varepsilon^2 + B_3\varepsilon^3 + B_4\varepsilon^4 + B_5\varepsilon^5 + B_6\varepsilon^6$$

$$\ln Z = C_0 + C_1\varepsilon + C_2\varepsilon^2 + C_3\varepsilon^3 + C_4\varepsilon^4 + C_5\varepsilon^5 + C_6\varepsilon^6$$

Z is Zener-Hollomon parameter;
ε is strain;
$\dot{\varepsilon}$ is strain rate;
A, n and α are material constants.

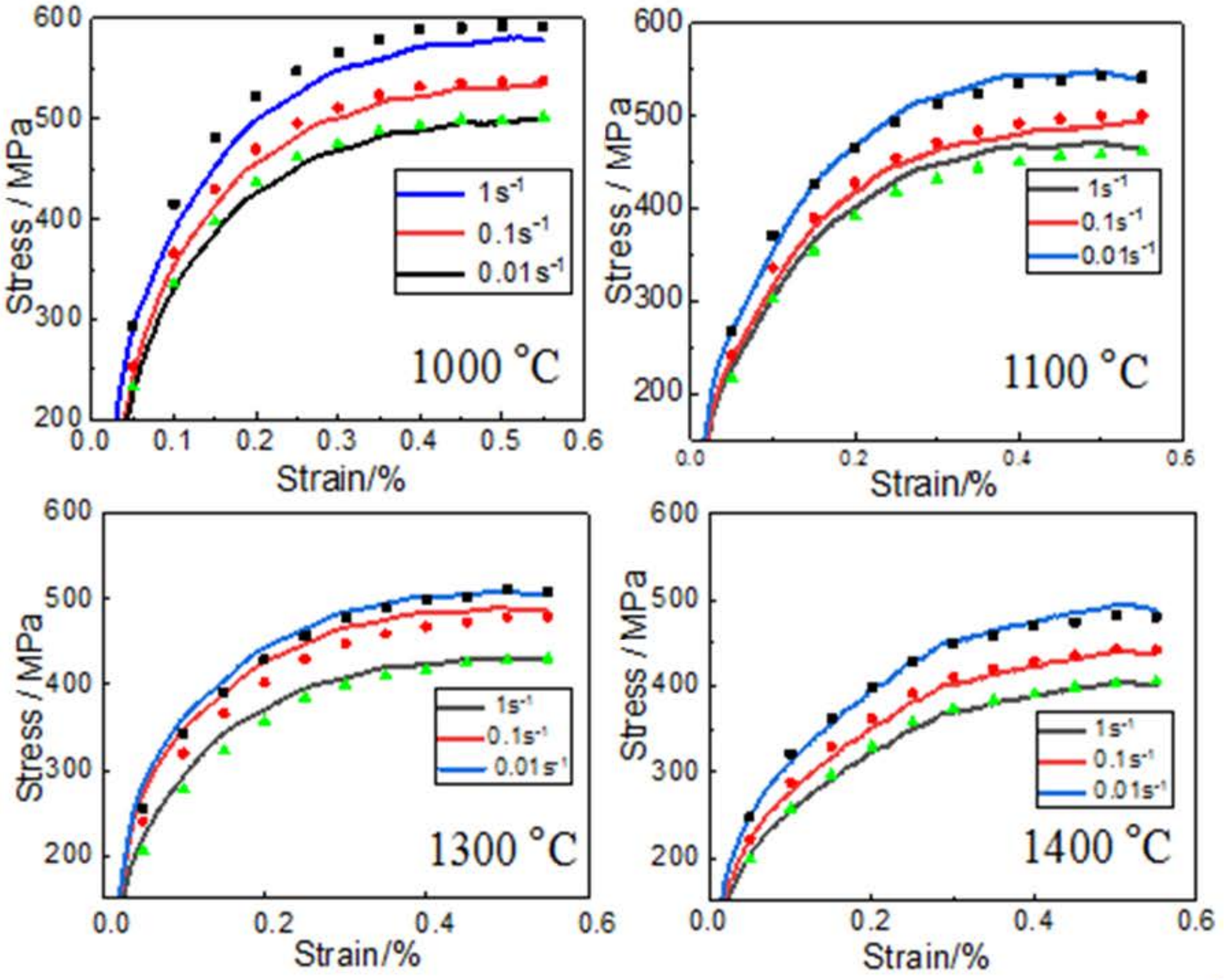

Conclusion: **The average relative error (AARE) = 3.6 % was calculated to investigate the good prediction accuracy.**

Conclusions

1. Investigation of reaction mechanism and formation mechanism of doped W precursor powders;
2. Development of an innovative liquid – liquid hydrothermal doping process;
3. Fabrication of W alloys having ZrO_2 particles (< 300 nm) within grains;
4. Fabrication of the advanced W alloys with high strength and critical failure strain.

Perspectives

1. **Tensile and bending tests at various temperatures (100 ~ 500 ℃);**
2. **Compressive tests at high temperatures (1000 ~ 1400 ℃);**
3. **Thermomechanical behaviour of the elaborated W alloys and numerical modelling;**
4. **Extension of the developed method for Y_2O_3, La_2O_3 and CeO_2 strengthened W alloy.**

Thank you for your attention!